ChemComm

Accepted Manuscript

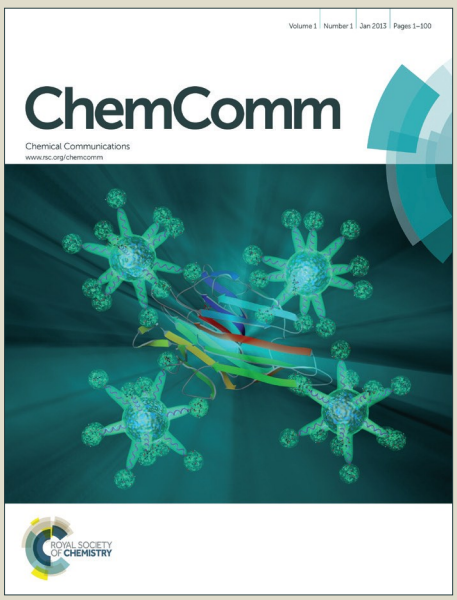

ROYAL SOCIETY OF CHEMISTRY

www.rsc.org/chemcomm

Journal Name

COMMUNICATION

Improved oxidation of aromatic and aliphatic hydrocarbons using rate enhancing variants of P450Bm3 in combination with decoy molecules

Received 00th January 20xx,
Accepted 00th January 20xx

DOI: 10.1039/x0xx00000x

www.rsc.org/

Samuel D. Munday,[a] Osami Shoji,[b] Yoshihito Watanabe,[b] Luet-Lok Wong[c] and Stephen G. Bell[a]*

Enzyme performance can be improved using decoy molecules or engineered variants to accelerate the activity without affecting selectivity. Here we combine a rate accelerator variant of cytochrome P450Bm3 with decoy molecules to enhance the oxidation activity of a range of small organic molecules. This combined approach offers superior biocatalytic efficiency without modifying the product distribution.

Cytochrome P450s (CYPs) are heme-dependent enzymes that catalyse the oxidation of a broad array of organic substrates, allowing them to perform physiological roles as varied as steroid hormone and antibiotic synthesis and the breakdown of xenobiotics.[1-3] The signature reaction of CYP enzymes is the insertion of a single oxygen atom from molecular dioxygen into a carbon–hydrogen bond to give the corresponding alcohol.[4] The direct hydroxylation of organic compounds by chemical methods is energy-intensive, often non-selective and leads to the formation of side products and toxic wastes. CYP-mediated oxidation reactions have the potential to provide efficient biocatalytic routes to alcohols by C–H activation, which is not feasible using classical organic synthetic methods.[5-8]

CYP102A1 (P450Bm3) from *Bacillus megaterium* is a soluble 119.5 kDa enzyme in which the P450 heme domain is fused to a reductase domain.[6] This catalytically self-sufficient enzyme requires only NADPH and oxygen to function, and hydroxylates medium-chain length (C_{11}–C_{18}) fatty acids at sub-terminal positions.[9] CYP102A1 and other CYP102 family enzymes exhibit the highest turnover frequency (> 1000 min^{-1}) of any CYP enzyme and this overcomes one of the major hurdles to the use of these enzymes in synthesis.[6,10] Wild-type P450Bm3 (WT) turns over most unnatural substrates at desultory rates but it is a versatile platform for designing biocatalysts via protein engineering.[5,6,11-15]

It has been shown that chemically inert perfluorocarboxylic acids (PFCs) can act as decoy molecules and greatly promote the oxidation of unnatural substrates such as benzenes and short chain alkanes. The inert decoy fills part of the P450Bm3 active site and constrains potential substrates to bind closer to the heme than they would without an added PFC, leading to increased activity.[15-17] The structure of a decoy molecule bound WT (PDB 3WSP) showed that the PFC filled the substrate channel but its shorter chain length left a significant amount of space close to the heme to bind another molecule (see ESI).[18] Enzyme-substrate interactions in the vicinity of the heme remain important in the catalytic activity.

An earlier directed evolution study identified P450Bm3 variants with enhanced activity for unnatural substrate oxidation but which maintained the product selectivity of the WT.[10,19-21] The crystal structure of the substrate-free form of the KT2 variant (A191T/N239H/I259V/A276T/L353I; PDB 3PSX) showed that it had the same conformation of the I helix around the critical oxygen-binding groove as fatty acid-bound WT.[21] The heme axial water interaction was weakened because the hydrogen bond between this water and the carbonyl of Ala264 was broken. This should promote substrate binding close to the heme. Kinetic studies also showed that the rate of the first electron transfer step for substrate-free KT2 was comparable to that of palmitic acid-bound WT. Therefore, KT2 has a catalytically ready conformation, such that substrate-induced changes to the structure play a less significant role in promoting the electron transfer steps (see ESI).[21]

Since the mechanisms by which decoy molecules and the KT2 variant showed enhanced unnatural substrate activity are different we explored whether these mechanisms would work in concert to facilitate the oxidation of smaller organic molecules such as benzene and cyclohexane by P450Bm3. We initially investigated the activity of WT P450Bm3 and the KT2 variant with and without added PFC8, PFC9 and PFC10.[18,22] As reported previously the addition of these PFCs improved the activity of the turnovers of WT P450Bm3 with cyclohexane and benzene.[22] These turnovers yielded phenol and cyclohexanol as the sole products. Both were identified by co-elution experiments with standards using GC-MS (Fig. 1 and Fig. S1). PFC10 itself induced the highest activity of NADPH oxidation in WT P450Bm3 followed by PFC9 and then PFC8 (Table 1 and ESI). This trend in NADPH oxidation activity was followed for the different PFC molecules. Addition of PFC9 increased the coupling efficiency with WT to a greater extent than PFC10 for both substrates (Table 1 and Fig. 1).[22] Overall the combined effects of increased activity and coupling resulted in the largest improvements in the product formation rate for PFC9 and PFC10

[a] *Department of Chemistry, University of Adelaide, SA 5005, Australia*
[b] *Department of Chemistry, Graduate School of Science, Nagoya University, Furo-cho, Chikusa-ku, Nagoya, 464-8602, Japan*
[c] *Department of Chemistry, University of Oxford, Inorganic Chemistry Laboratory, South Parks Road, Oxford, OX1 3QR, UK*
** To whom correspondence should be addressed. stephen.bell@adelaide.edu.au*
Electronic Supplementary Information (ESI) available: [Experimenal, Structure details, NADPH consumption traces, MS data, GC-MS and HPLC analysis). See DOI: 10.1039/x0xx00000x

Table 1 *In vitro* turnover activity data for the P450Bm3 variants and decoy molecule combinations with benzene and cyclohexane as substrates and in the absence of substrate (decoy). N = NADPH turnover rate. C = coupling efficiency (%). PFR = product formation rate. Rates are in nmol.(nmol-P450)$^{-1}$.min^{-1}. All data are reported as mean ± S.D. (n>3).

	decoy	benzene			cyclohexane		
	N	N	C	PFR	N	C	PFR
WT	-	29 ± 0.3	0.6 ± 0.05	0.2 ± 0.02	30 ± 2	2.2 ± 0.4	0.7 ± 0.07
WT/PFC8	35 ± 1	71 ± 1	3.0 ± 0.2	2 ± 0.2	212 ± 8	31 ± 2	65 ± 6
WT/PFC9	56 ± 0.4	168 ± 7	13 ± 0.6	23 ± 1	416 ± 7	28 ± 2	119 ± 8
WT/PFC10	327 ± 11	522 ± 6	8.6 ± 0.6	45 ± 4	626 ± 14	15 ± 1	91 ± 7
KT2	-	77 ± 6	3.0 ± 0.2	2.3 ± 0.3	353 ± 9	19 ± 1	70 ± 5
KT2/PFC8	83 ± 3	220 ± 4	4.6 ± 0.4	10 ± 1	900 ± 19	35 ± 4	315 ± 36
KT2/PFC9	161 ± 8	374 ± 7	10 ± 0.3	38 ± 1	1338 ± 25	36 ± 1	483 ± 28
KT2/PFC10	699 ± 12	847 ± 10	8.8 ± 0.8	74 ± 1	1797 ± 45	27 ± 1	484 ± 31

over PFC8 (Table 1). The maximal augmentation of the activity upon addition of a decoy molecule was 170-fold for cyclohexane and 225-fold for benzene.

In the absence of added PFCs the KT2 variant showed increased NADPH oxidation activity, coupling efficiency and hence the product formation rate over the WT with both benzene and cyclohexane, in line with what has been reported previously with other substrates (Table 1 and Fig. 1).[10, 21] Benzene oxidation was 12-fold faster and a 100-fold increase was observed for cyclohexane. However, the activities were lower than the best WT/PFC combinations (Table 1). Addition of the PFC decoy molecules to KT2 engendered further enhancement of the oxidation of benzene and cyclohexane. The activity was higher than with the WT in all cases. The trends in the catalytic parameters of the different PFCs with KT2 mirrored those obtained with the WT (Table 1). As a consequence the product formation rate of KT2 with PFC9 and PFC10 are similar and both are greater than when PFC8 is used. KT2 and PFC10 was the most active combination for benzene oxidation, with a product formation rate

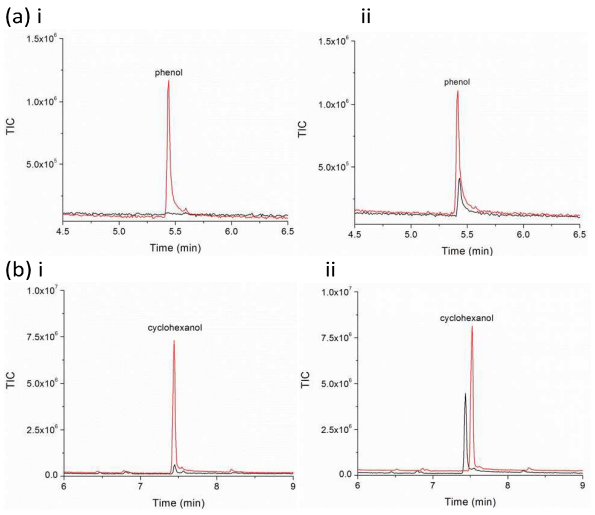

Fig. 1 GC-MS analysis of the turnovers of (a) benzene and (b) cyclohexane using the WT (i) and KT2 (ii) variants of P450Bm3 with and without the decoy molecule PFC9. In black is the turnover in the absence of the decoy molecule and in red the turnover in the presence of the decoy molecule. In (b) (ii) the turnover of cyclohexane with KT2 with PFC9 has been offset slightly along the x-axis for clarity. The integrations of these peaks and the internal standard are given in Table S1.

of 74 min^{-1}. The gain in activity with cyclohexane was even greater, with the product formation rate being 484 min^{-1} and 483 min^{-1} with the KT2/PFC10 and KT2/PFC9 combinations. This was four-fold higher than the best WT pairing (PFC9, Table 1 and Fig. 1).

Encouraged by these results we assessed if the decoy molecule/rate enhancement mutant combinations would work for substituted benzenes. The oxidation of toluene and anisole by P450Bm3 have been reported to be highly selective (>90%) for the *ortho*-hydroxylated product.[21-23] The turnovers of toluene generated *p*-cresol with benzyl alcohol as a minor product (<9% total product) while 4-methoxyphenol (<10%) is the sole minor product identified for anisole oxidation.[22,23] The biocatalytic oxidation of xylenes by P450Bm3 has also been reported. The turnover of *p*-xylene is documented to generate only 2,5-dimethylphenol[24] and *m*-xylene oxidation produced 2,4-dimethylphenol (87%), 2,6-dimethylphenol (11%) and 3-methylbenzylalcohol (2%).[25] The P450Bm3 catalysed oxidation of *o*-xylene was more complex, yielding five products. The major product is 2-methylbenzyl alcohol (47%) with 2,3- and 3,4-dimethylphenol being generated as two of the minor products, 27% and 10%, respectively. The other two minor metabolites arise from a methyl shift resulting in formation of 2,6-dimethylphenol (8%) and the dearomatisation product, 6,6-dimethylcyclohexa-2,4-dienone (8%, Scheme 1).[25] The analysis of the turnovers of these larger substrates with the PFCs and KT2 would be a more stringent test to assess if these mutant and decoy molecule combinations would alter the product distribution as well as heighten the activity.

All five substrates were tested with WT and KT2 P450Bm3 with PFC8 through to PFC10. Despite the larger size of these substituted benzenes, a similar pattern of activity enhancement was observed with the decoy molecules. The turnovers containing PFC10 showed the highest activity of NADPH oxidation and those with PFC9 were the more efficiently coupled. In certain instances, e.g. with toluene, the faster rates of NADPH oxidation with PFC10 resulted in higher product formation rates while in others the higher coupling obtained with PFC9 resulted in the maximum activity, e.g. *p*-xylene with KT2/PFC9 (Table 2). In all cases the greatest product formation rates were obtained with KT2/PFC9 or KT2/PFC10.

The oxidation of both toluene and anisole was faster than that of benzene for all the enzyme/decoy molecule combinations tested. The maximum enhancements in the rate of product formation, over WT P450Bm3, were approximately 900-fold for toluene and 40-fold for anisole (Table 2 and Table S2). The larger gain with toluene predominantly arose from a more significant increase in the coupling efficiency when compared to the anisole turnovers.

Table 2 *In vitro* turnover activity data for the P450Bm3 variants and decoy molecule combinations with toluene, anisole, *p*-, *m*- and *o*-xylene. See Table 1 for details.

	WT	WT +PFC9	WT +PFC10	KT2	KT2 +PFC9	KT2 +PFC10
Toluene						
N	22 ± 0.9	355 ± 3	622 ± 8	68 ± 2	549 ± 7	822 ± 12
C	1.6 ± 0.5	40 ± 1	25 ± 2	9.7 ± 3	41 ± 1	33 ± 1
PFR	0.3 ± 0.1	144 ± 3	158 ± 10	7 ± 2	225 ± 8	271 ± 9
anisole						
N	122 ± 2	262 ± 2	581 ± 3	189 ± 12	399 ± 9	729 ± 16
C	1.4 ± 0.1	18 ± 3	11 ± 0.5	7.5 ± 1	19 ± 2	12 ± 0.1
PFR	2.0 ± 0.1	48 ± 9	64 ± 3	14 ± 2	76 ± 6	87 ± 2
***p*-xylene**						
N	63 ± 5	687 ± 7	943 ± 7	267 ± 10	1010 ± 33	1080 ± 8
C	19 ± 2	56 ± 4	41 ± 4	34 ± 0.9	54 ± 2	42 ± 2
PFR	12 ± 2	386 ± 26	394 ± 35	90 ± 1	549 ± 22	460 ± 26
***m*-xylene**						
N	33 ± 0.6	546 ± 3	698 ± 8	178 ± 5	830 ± 7	1050 ± 12
C	3.5 ± 0.4	55 ± 1	40 ± 0.4	26 ± 2	57 ± 2	43 ± 2
PFR	1.1 ± 0.1	302 ± 5	278 ± 4	46 ± 4	476 ± 15	455 ± 12
***o*-xylene**						
N	29 ± 1	284 ± 5	468 ± 5	106 ± 2	738 ± 18	1020 ± 16
C	1.9 ± 0.1	53 ± 2	28 ± 2	30 ± 3	45 ± 1	34 ± 1
PFR	0.6 ± 0.06	149 ± 8	131 ± 6	32 ± 2	334 ± 17	346 ± 10

The best KT2/PFC combinations resulted in product formation rates which were almost double that of the WT/PFC pairings. The oxidation of toluene and anisole resulted in the generation of *o*-cresol (94–95%) and *o*-methoxyphenol (88–92%), respectively (Fig. S2, S3 and Table S3). Benzyl alcohol and *p*-cresol from toluene and 4-methoxyphenol from anisole were minor metabolites in these turnovers. The product distributions were virtually unchanged when compared to the WT enzyme (Scheme 1, Fig. S2, Table S3).

Xylene oxidation was enhanced using the PFC decoys with KT2. The maximum activity enhancements over the WT were; *p*-xylene, 45-fold; *m*-xylene, 430-fold; *o*-xylene, 575-fold (Table 2 and Fig, S4). The product formation rates were higher than those achieved with toluene. The product distributions across all the turnovers were comparable to those reported for the WT and the KT2 variant (Scheme 1, Fig. S2 and S3, Table S3). For example, the ratios of the five products formed by the WT enzyme and *o*-xylene, including those arising from a shift in a methyl group, are similar to those obtained with the KT2/PFC10 combination, which has the highest activity (Fig. 2 and Table S3).

One point of difference to the previously reported data for *p*-xylene was that three products were observed in the GC-MS analysis of all the turnovers including those of the WT enzyme (Fig. 2, Fig. S5 and Table S3).[24] These corresponded to 4-methylbenzyl alcohol (0–6%), 2,4- and 2,5-dimethylphenol (15–17% and 77–85%, respectively). The 2,4-dimethylphenol product must arise via the NIH shift of a methyl group an activity that is also observed with *o*-xylene (Scheme S1).[25]

The rate enhancement for KT2/PFC combinations over the WT/PFC counterparts arose mainly from increased NADPH oxidation activity rather than enhanced coupling (Tables 1 & 2). In addition, the regioselectivity was unchanged when PFCs were added to the WT or KT2. These observations are consistent with the catalytically ready structure of the KT2 variant, pre-disposing it to electron transfer, with little effect on substrate binding orientation and product selectivity. The PFC decoys, on the other hand, fill part of the active site and constrain the substrate to bind closer to the heme. This is a determining factor for enhanced coupling but the PFC does not interfere with substrate binding close to the heme

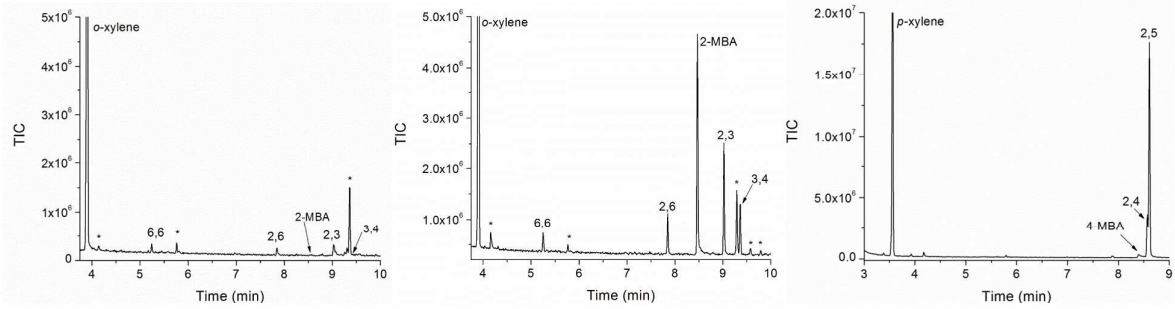

(a) i (a) ii b)

Fig. 2 GC-MS analysis of the turnovers of (a) *o*-xylene using (i) WT P450Bm3 and (ii) KT2 and PFC10, the products are labelled; 2-methylbenzylalcohol (2-MBA), 2,3-dimethylphenol (2,3), 3,4-dimethylphenol (3,4), 2,6-dimethylphenol (2,6), and 6,6-dimethylcyclohexa-2,4-dienone (6,6).(b) (i) *p*-xylene using the KT2 and PFC8, the products are labelled 2,5-dimethylphenol (2,5), 2,4-dimethylphenol (2,4) and 4-methylbenzyl alcohol (4-MBA) Impurities are labelled *.

which determines the regioselectivity. For substituted benzenes the phenol product formed is dependent on the carbocation stability during NIH shift rearrangement of the arene oxide intermediates rather than the proximity of arene C–H bonds to the ferryl oxygen.

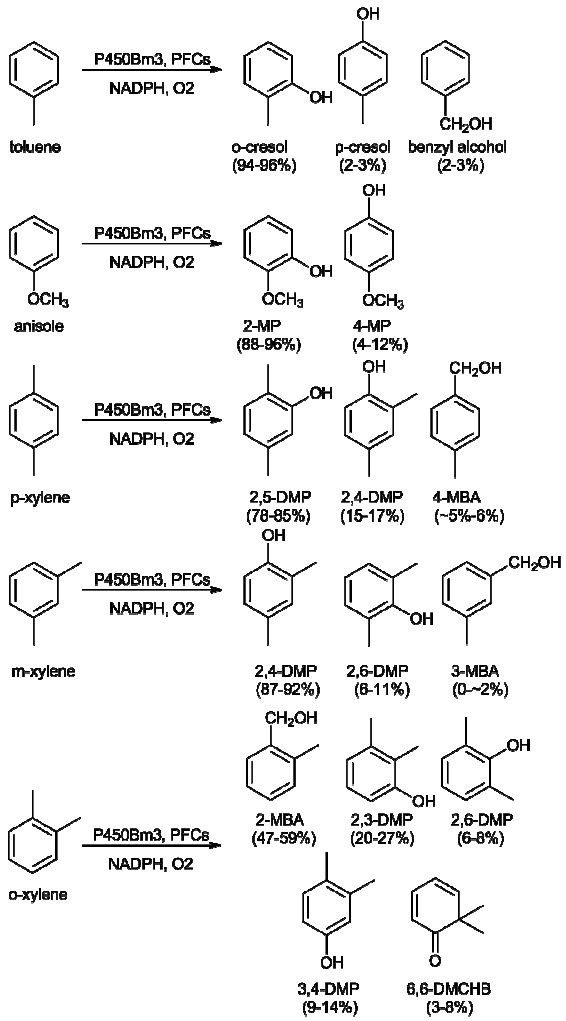

Scheme 1 The products formed from the turnovers of P450Bm3 enzyme/decoy molecule combinations with benzene substrates. Abbreviations used; 2-methoxyphenol (2-MP), 4-methoxyphenol (4-MP), 2,5-dimethylphenol (2,5-DMP), 2,4-dimethylphenol (2,4-DMP), 4-methylbenzyl alcohol (4-MBA), 2,6-dimethylphenol (2,6-DMP), 3-methylbenzylalcohol (3-MBA), 2-methylbenzylalcohol (2-MBA), 2,3-dimethylphenol (2,3-DMP), 3,4-dimethylphenol (3,4-DMP) and 6,6-dimethylcyclohexa-2,4-dienone (6,6-DMCHD).

In conclusion we have shown that the combination of a rate accelerating mutant and a decoy molecule is a simple and efficient method to improve the activity of P450Bm3 without altering the product distribution. The improvements were greatest for cyclohexane and the KT2/PFC decoy molecule combinations seem to be well suited for the oxidation of smaller alkanes. This approach provides additional evidence for multiple binding sites in P450Bm3[26] and could be used to drive substrate oxidation by CYP enzymes at high activities and improved product yields. This would enable the generation of the levels of product required in synthetic chemistry applications for reactions which show promising regio- and stereoselectivity with WT or mutant forms of the enzyme.

The authors thank the University of Adelaide for the award of a M. Phil Scholarship (to SDM) and part-funding the project through the award of a Priority Partner Project Grant (with Nagoya University).

Notes and references

1 P. R. Ortiz de Montellano, *Cytochrome P450: Structure, Mechanism and Biochemistry*, Plenum Publishers, New York, **2005**.
2 A. Sigel, H. Sigel and R. Sigel, *The Ubiquitous Roles of Cytochrome P450 Proteins*, John Wiley & Sons, Weinheim, **2007**.
3 F. P. Guengerich, *Chem. Res. Toxicol.*, 2001, **14**, 611-650.
4 P. R. Ortiz de Montellano, *Chem. Rev.*, 2010, **110**, 932-948.
5 S. G. Bell, N. Hoskins, C. J. C. Whitehouse and L. L. Wong, *Met. Ions Life Sci.*, **2007**, 437-476.
6 C. J. Whitehouse, S. G. Bell and L. L. Wong, *Chem. Soc. Rev.*, 2012, **41**, 1218-1260.
7 G. D. Roiban and M. T. Reetz, *Chem. Commun.*, 2015, **51**, 2208-2224.
8 R. Fasan, *ACS Catalysis*, 2012, **2**, 647-666.
9 S. S. Boddupalli, R. W. Estabrook and J. A. Peterson, *J Biol. Chem.*, 1990, **265**, 4233-4239.
10 C. J. Whitehouse, S. G. Bell, H. G. Tufton, R. J. Kenny, L. C. Ogilvie and L. L. Wong, *Chem. Commun.*, 2008, 966-968.
11 A. Seifert, S. Vomund, K. Grohmann, S. Kriening, V. B. Urlacher, S. Laschat and J. Pleiss, *Chembiochem*, 2009, **10**, 853-861.
12 J. A. McIntosh, P. S. Coelho, C. C. Farwell, Z. J. Wang, J. C. Lewis, T. R. Brown and F. H. Arnold, *Angew. Chem. Int. Ed. Engl.*, 2013, **52**, 9309-9312.
13 S. Kille, F. E. Zilly, J. P. Acevedo and M. T. Reetz, *Nat. Chem.*, 2011, **3**, 738-743.
14 G. Di Nardo and G. Gilardi, *Int. J. Mol. Sci.*, 2012, **13**, 15901-15924.
15 O. Shoji, T. Fujishiro, H. Nakajima, M. Kim, S. Nagano, Y. Shiro and Y. Watanabe, *Angew. Chem. Int. Ed. Engl.*, 2007, **46**, 3656-3659.
16 N. Kawakami, O. Shoji and Y. Watanabe, *Angew. Chem. Int. Ed. Engl.*, 2011, **50**, 5315-5318.
17 F. E. Zilly, J. P. Acevedo, W. Augustyniak, A. Deege, U. W. Hausig and M. T. Reetz, *Angew. Chem. Int. Ed. Engl.*, 2011, **50**, 2720-2724.
18 Z. Cong, O. Shoji, C. Kasai, N. Kawakami, H. Sugimoto, Y. Shiro and Y. Watanabe, *ACS Catalysis*, 2015, **5**, 150-156.
19 C. J. Whitehouse, S. G. Bell, W. Yang, J. A. Yorke, C. F. Blanford, A. J. Strong, E. J. Morse, M. Bartlam, Z. Rao and L. L. Wong, *Chembiochem*, 2009, **10**, 1654-1656.
20 C. J. Whitehouse, W. Yang, J. A. Yorke, B. C. Rowlatt, A. J. Strong, C. F. Blanford, S. G. Bell, M. Bartlam, L. L. Wong and Z. Rao, *Chembiochem*, 2010, **11**, 2549-2556.
21 C. J. Whitehouse, W. Yang, J. A. Yorke, H. G. Tufton, L. C. Ogilvie, S. G. Bell, W. Zhou, M. Bartlam, Z. Rao and L. L. Wong, *Dalton Trans.*, 2011, **40**, 10383-10396.
22 O. Shoji, T. Kunimatsu, N. Kawakami and Y. Watanabe, *Angew. Chem. Int. Ed. Engl.*, 2013, **52**, 6606-6610.
23. A. Dennig, N. Lulsdorf, H. Liu and U. Schwaneberg, *Angew. Chem. Int. Ed. Engl.*, 2013, **52**, 8459-8462.
24 A. Dennig, J. Marienhagen, A. J. Ruff, L. Guddat and U. Schwaneberg, *ChemCatChem*, 2012, **4**, 771-773.
25 C. J. Whitehouse, N. H. Rees, S. G. Bell and L. L. Wong, *Chem. Eur. J.*, 2011, **17**, 6862-6868.
26. B. Rowlatt, J. A. Yorke, A. J. Strong, C. J. Whitehouse, S. G. Bell and L. L. Wong, *Protein Cell*, 2011, **2**, 656-671.